Temperature-Dependent Behavior of the Dual Fluorescence of 2-(3-Fluorophenyl)-2,3-dihydro-1*H*-benzo[*f*]isoindole-1,3-dione

by **Pierre Valat**, **Véronique Wintgens**, and **Jean Kossanyi***

C.N.R.S., 2–8 rue Henri Dunant, F-94320 Thiais (e-mail: kossanyi@glvt-cnrs.fr)

and **Làszlò Biczòk**, **Attila Demeter**, and **Tibor Bérces**

Institute of Chemistry, Chemical Research Center, Hungarian Academy of Sciences, Pusztaszeri ut 59–67, H-1025 Budapest

Dedicated to Prof. *André M. Braun* on the occasion of his 60th birthday

The fluorescence behavior of 2-(3-fluorophenyl)-2,3-dihydro-1*H*-benzo[*f*]isoindole-1,3-dione (**1**) was studied in solvents of different polarity and viscosity. Dual luminescence is observed and the short-wavelength emission is found to increase considerably with the solvent polarity. The ratio of the fluorescence quantum yield of the two states emitting, the one (SW*) at short wavelength and the other (LW*) at long wavelength, shows a bell-shaped dependence on the reciprocal of the temperature in diethyl ether, butyronitrile, and propane-1,2,3-triol triacetate (glycerol triacetate; GTA). This has been interpreted as the result of a reversible interconversion between the two states. The enthalpy difference between the SW* and LW* excited states, as deduced from the slope of the $\ln(\Phi_f^{LW}/\Phi_f^{SW})$ *vs.* $1/T$ curves in the high temperature range, is found to be solvent polarity and solvent viscosity independent as the same value (– 7.3 kJ/mol) is obtained in the three above-mentioned solvents. The independence from polarity is the consequence of a similar difference in dipole moment between the ground-state and the SW* and LW* excited states (4.5 and 4.9 D, respectively, derived from solvatochromy). The activation energy of the SW* → LW* step deduced from the low temperature measurements in the nonviscous solvents, increases with solvent polarity (11.6 and 17.5 kJ/mol for diethyl ether and butyronitrile, respectively); they are greater than the viscous-flow activation energy of the solvents indicating that the resolvation of the excited dipole controls the kinetics. In the nonviscous solvents, the LW* state originates from the SW* state, while in the viscous GTA solution, both states are formed simultaneously within the 1-ps laser pulse.

1. Introduction. – Naphthalene-dicarboximides have received in the past few years considerable attention for both their spectroscopic properties and their potential applications in biology. For instance, they can intercalate at specific positions of DNA and induce a photocleavage of the DNA doublehelix [1–3]. One derivative has also been shown to present antineoplastic activities against mouse *Ehrlich* ascites and *in vitro* cytotoxic activity against HeLa cells [4–6]. Upon irradiation, other compounds of the series not only inactivate enveloped viruses and cells, but also inhibit the formation of syncytium by HIV-1-infected cells [7–9]. Such properties explain the increased interest in the characterization of the photophysical properties of the compounds of this family.

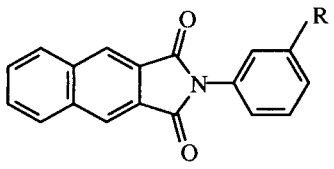

1 R = F
2 R = H

In a previous publication, we reported [10] on the spectroscopic and photophysical properties of a series of phenyl-substituted 2,3-dihydro-2-phenyl-1*H*-benz[*f*]isoindole-1,3-dione, **2** and pointed out the importance of the electron-donating character of the substitution to the fluorescence of the molecule. Observations made with the unsubstituted molecule **2** indicated [11] that, under certain conditions, dual luminescence can be observed, with an emission at long-wavelength (named hereafter 'long-wavelength' (LW) fluorescence), which appears well-separated and red-shifted from the so-called 'short-wavelength' (SW) emission. These two emissions differ from each other not only by their position, but also by their decay. When no SW* → LW* transformation is observed, as in the case of **2** [11], the relaxed SW* emission decays in the picosecond time range and the LW* emission in the nanosecond time scale. This behavior differs *i*) from the usual case [12–17], where the SW* state is the precursor of the LW* state and also *ii*) from the classical excimer formation [18–21]. Substitution of the *N*-phenyl ring with electron donors yields a broad long-lived LW* fluorescence [10], while electron acceptors enhance the emission of the SW* state. For the *m*-fluoro derivative **1** (and for a few others) the LW* state has been found to revert to the SW* state [10]. The aim of the present article is to settle the difference between the metafluoro-substituted naphthalimide **1** and the unsubstituted **2**, to confirm the reversibility between the two singlet excited states of **1**, and to explain the change of its spectroscopic properties with the polarity and viscosity of the medium.

2. Experimental. – Compound **1** was prepared according to the procedure described in [10].

AcOEt (*Prolabo*, HPLC grade), MeCN (*Prolabo*, HPLC grade), butyronitrile (*Aldrich*, spectroscopy grade), and Et_2O (*Fluka*, spectroscopy grade) were used as received. Propane-1,2,3-triol triacetate (glycerol triacetate; GTA; *Prolabo*, RP) was distilled under reduced pressure above anh. Na_2CO_3 and checked for the absence of fluorescent impurities.

The UV-VIS absorption spectra were obtained with a *Varian-Cary 219* spectrophotometer. Fluorescence spectra were recorded with a *SLM-Aminco 8000* spectrofluorometer. Fluorescence quantum yields were determined in O_2-free solution by comparison with the emission of **2** in deoxygenated MeCN solution, for which the value of $\Phi_f = 0.27$ had been measured [22]. The fluorescence spectra were deconvoluted by modelling the LW* emission with a gaussian curve on a cm^{-1} scale, and subtracting it from the measured curve. The resulting SW* emission is very similar to that obtained for the model compound 2,3-dihydro-2-methylbenzo[*f*]isoindole-1,3-dione in the same medium [22].

Fluorescence decays were measured by excitation with a frequency-tripled pulsed YAG laser (*B. M. Industries*) with a 30 ps full width at half maximum (FWHM) according to the experimental set-up described in [23]. The resolution of the experimental set-up was limited by the 0.3 ns start-up time of the oscilloscope.

Variable-temperature measurements in the 270–335 K range were carried out with a home-made temperature-regulated cell holder equipped with an external circulating bath. The temperature of the sample was measured directly inside the cell. Low-temperature measurements (in the 80–295 K range) were carried out with a liq. N_2-cooled cryostat from *Oxford Instruments*.

The experiments under pressure were carried out[1]) in a 0.8×0.8 cm quartz cuvette at 25° with a 0.5 cm optical path. This cell is fixed in a metal cell holder that permits the cell to be closed with a thin *Teflon* membrane to isolate the test soln. from the compression fluid. The cell is immersed in a high pressure bomb made of specially treated metal (*Marval X12*). The geometry of the bomb is a modified version of that previously described [24][25], comprised of four sapphire windows at right angles to the geometry of the *SLM-Aminco* Spectrofluorimeter. One aperture perpendicular to the windows on top of the bomb is designed for the introduction and alignment of the optical cell inside the bomb. The bomb itself is immersed in a thermostated fluid (EtOH) contained in a thermally insulated box. Thermal regulation of the fluid at $25 \pm 0.1°$ is provided by a *HS40* thermostated circulating bath.

---

[1]) We thank Dr. *G. Hui Bon Hoa*, Institut de Biologie Physico-Chimique, Paris, France, for his help with these measurements.

3. Results. – 3.1. *Influence of Solvent Polarity.* The position of both SW and LW fluorescence bands (*Fig. 1*) is red-shifted by 700 and 880 cm^{-1}, respectively, when the solvent is changed from Et_2O ($\varepsilon = 4.3$) to MeCN ($\varepsilon = 37.5$). At the same time, the fluorescence quantum yield of the LW state almost does not change and decays only little (within experimental errors) from one solvent to the other. The situation is quite different with the SW state for which the fluorescence quantum yield increases steadily with the solvent polarity (*Fig. 1*) and changes by one order of magnitude (*Table 1*) between hexane and MeCN.

The small *Stoke*'s shift observed for the fluorescence spectra of **1** in solvents of different polarity (*Fig. 1*) is consistent with a small change of the excited-state dipole

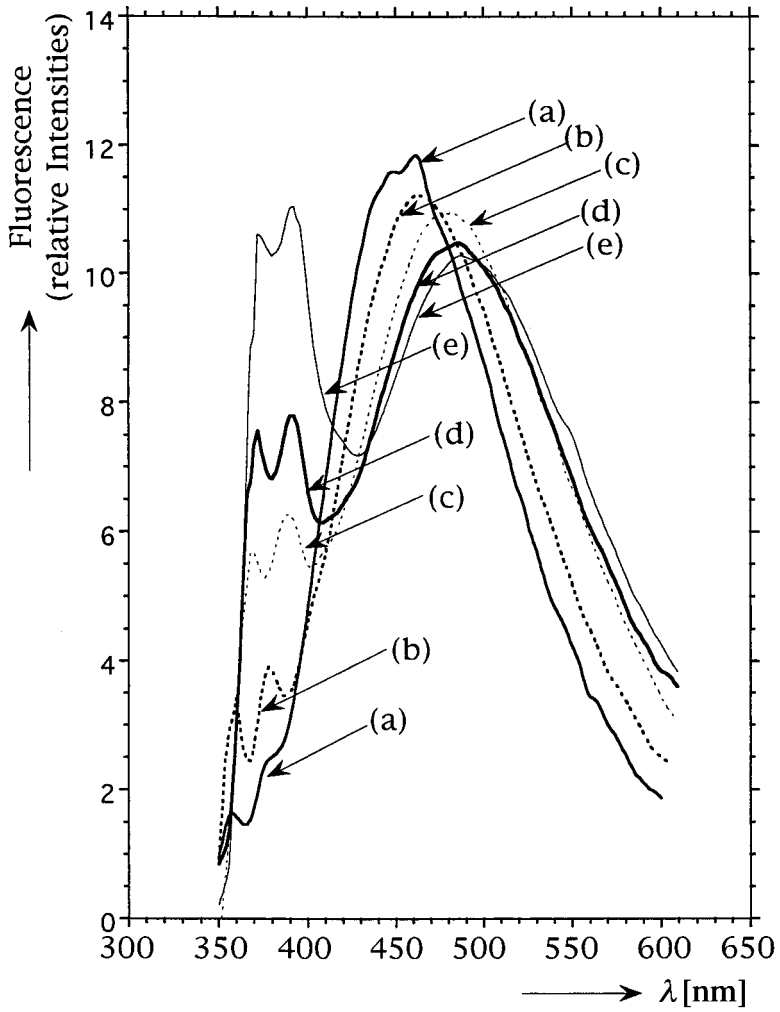

Fig. 1. *Fluorescence emission of* **1** *in solvents of different polarities:* a) *hexane,* b) *Et_2O,* c) *AcOEt,* d) *butyronitrile, and* e) *MeCN*

Table 1. *Absorption Maximum, and SW** (highest vibrational-energy level) *and LW* Fluorescence-Band Maxima, and Fluorescence Quantum Yields of* **1** *in Different Solvents*

Solvent	ε	λ_{max}^{abs} [nm]	λ_{max}^{LW} [nm]	Φ_f^{LW} [$\times 10^3$]	λ_{max}^{SW} [nm]	Φ_f^{SW} ($\times 10^3$)	$\frac{\Phi_f^{LW}}{\Phi_f^{SW}}$	τ_{LW} [ns]
MeCN	37.5	358	487	8.6	373.5	2.4	3.6	1.68
Butyronitrile	19	357.5	483	8.8	370.5	1.6	5.5	1.76
AcOEt	6.2	356.5	475	9.1	369	1.1	8.3	1.64
Et_2O	4.3	356	467	8.4	363.5	0.61	13.7	1.55
Hexane	0.0	354	457	7.0	357	0.24	29.1	1.25

moment compared to that of the ground state. This excludes an intramolecular charge transfer with full electron shift, which would have been stabilized by the reorientation relaxation of a highly polar solvent. The change in dipole moment $\Delta\mu$ between the ground-state and the SW* and LW* excited states has been calculated from the position of the absorption ($\bar{\nu}_a$) and fluorescence ($\bar{\nu}_f$) maxima by means of the *Lippert-Mataga* expresssion [26][27]:

$$\Delta\bar{\nu} = \bar{\nu}_a - \bar{\nu}_f = \frac{2(\Delta\mu)^2}{hca^3}\left[\frac{\varepsilon - 1}{2\varepsilon + 1} - \frac{n^2 - 1}{2n^2 + 1}\right]$$

where h, c, and a correspond to the Planck constant (6.62×10^{-34} J), the velocity of light in the vacuum (2.99×10^8 m/s) and the equivalent spherical radius of the solute assimilated to the solvent cavity in the *Kirkwood-Onsager* continuum model, respectively; ε is the dielectric constant of the solvent and n its refractive index. The value $a = 4.1$ Å is calculated from tabulated atomic increments [28]. The slope of the linear plot of ($\bar{\nu}_a - \bar{\nu}_f$) *vs.* Δf, equal to 3062 cm^{-1} for SW* and 3612 cm^{-1} for LW*, leads to the value of 4.5 D and 4.9 D for the change in dipole moment ($\Delta\mu$) of the SW* and LW* excited states, respectively, in reference to their ground states.

3.2. *Influence of Solvent Viscosity.* The steep temperature and pressure dependence of the viscosity of GTA solution was used to examine the effect of the solvent viscosity on the spectroscopic properties of **1**.

One set of experiments was carried out in GTA over a small temperature range (273 to 293 K) so that any change originating from an *Arrhenius*-type energy barrier would be neglected. First, experiments were carried out in AcOEt, a solvent of polarity ($\varepsilon = 6.02$) close to that of GTA ($\varepsilon = 7.11$) but of low viscosity, 0.46 cP and 28 cP, respectively, at 290 K. In AcOEt, the SW* emission increases moderately (by *ca.* 10%) while the LW* emission increases by more than 25% when the temperature is decreased from 293 to 273 K. The postion of the two bands remains practically unchanged over this temperature range.

In the viscous GTA solution at room temperature and under atmospheric pressure, the short-wavelength fluorescence is already three times more intense than in the nonviscous AcOEt medium, and its intensity increases by a factor of two when the temperature is decreased from 293 to 273 K. The inensity of the LW fluorescence band varies only little (it increases by *ca.* 10%) during this temperature change and, as in AcOEt, the positions of the two bands do not change within this small temperature change. The decay of the LW* emission slows from 2.05 ns to 2.28 ns within this 20 K decrease. Three additional observations could be made in the present case: *i*) the SW*

fluorescence decays biexponentially with a short-lived component in the picosecond time scale and a long-lived component in the ns time scale; *ii*) the decay of the long-lived component of the SW* emission is the same as that of the long-wavelength fluorescence; *iii*) the contribution of the short-lived component to the decay of the SW* fluorescence increases markedly when the temperature decreases.

The second type of experiment was carried out in GTA with an increase in pressure above the solution. Then, when the pressure was increased from 1 bar to 5 kbar, the intensity of the LW* emission decreased by less than 10% while that of the SW* fluorescence increased [29] by a factor of 40.

3.3. *Influence of Temperature.* Three different effects are expected from the temperature decrease: first, it reduces the rate of thermally activated processes; second, it increases the polarity of the solvent [30][31]; third, it increases the viscosity of the medium and, therefore, hinders the rotational movement of the molecules and reduces the solvent reorganization process. According to the above-described experiments carried out under high pressure, the effect of viscosity is noticeable only for high viscosity values. As a consequence, a limited or no viscosity effect is expected in Et_2O or butyronitrile. The small shift in the position of the fluorescence bands, and the limited variation in dipole moment between the ground-state on one side and the SW* and LW* excited states on the other side, indicate that the influence of the solvent polarity is negligible. Consequently, the thermally activated processes in these two solvents can be characterized by examining *i*) the variation of the fluorescence quantum yield at short and long wavelengths and *ii*) the decay of the emitting excited states.

Two solvents, one of relatively high polarity (butyronitrile, $\varepsilon = 19$, measurements at 283 – 168 K) and the other of low polarity (Et_2O, $\varepsilon = 4.3$, measurements at 300 – 159 K) have been used for the temperature-dependence experiments. With both solvents, the results were corrected for a slight variation in the optical density of the sample at the excitation wavelength. Additional experiments in the highly viscous solvent GTA were performed in the 313 – 253 K temperature range for comparison (*vide infra*).

3.3.1. *Butyronitrile Solution.* In this solvent, the decay of the SW* and LW* emissions can be measured independently. At the short-wavelengths, the fluorescence decays biexponentially and the importance of its short-lived (< 300 ps) component increases regularly as the temperature is decreased. On the other hand, the decay of the long-lived component is identical (in the ns time scale) to the decay at the long-wavelengths. Due to the limited time resolution (> 300 ps) of the experimental set-up used, no development of the LW emission could be detected. The decay of the LW* state as well as that of the long-lived component of the SW* state (*Table 2*), slows down continuously from 2.0 ns at 283 K to 2.9 ns at 168 K.

The LW* state fluorescence quantum yield also increases while that of the SW* state first decreases, reaches a minimum at a temperature of about 220 K, and begins to increase again below this temperature (*Table 2*).

As deduced from *Fig. 2*, the position of the two fluorescence bands in the polar butyronitrile solution appears to be independent of the temperature.

Table 2 gives the values of the fluorescence quantum yield of the two emissions, of their ratio as well as the decay (τ_{LW}) of the LW emission at the different temperatures. In addition, the logarithm of the fluorescence quantum-yield ratio, ln (Φ_f^{LW}/Φ_f^{SW}), has been plotted *vs.* the reciprocal of the absolute temperature (*Fig. 3*).

Table 2. *Fluorescence Data of* **1** *in Butyronitrile Solution at Various Temperatures*

$10^3/T$	Φ_f^{LW} ($\times 10^3$)	$\ln \Phi_f^{LW}$	Φ_f^{SW} ($\times 10^3$)	$\ln \Phi_f^{SW}$	$\frac{\Phi_f^{LW}}{\Phi_f^{SW}}$	$\left(\ln \frac{\Phi_f^{LW}}{\Phi_f^{SW}}\right)$	τ_{LW} [ns]
3.53	8.11	– 4.81	1.14	– 6.78	7.11	1.96	2.02
3.73	8.10	– 4.82	0.88	– 7.04	9.2	2.22	2.10
3.95	8.50	– 4.77	0.78	– 7.16	10.9	2.39	
4.20	8.52	– 4.76	0.70	– 7.26	12.17	2.50	2.32
4.48	8.55	– 4.76	0.61	– 7.40	14.02	2.64	2.43
4.81	8.65	– 4.75	0.62	– 7.39	13.95	2.64	2.53
5.32	8.86	– 4.73	0.94	– 6.97	9.43	2.24	2.72
5.62	9.10	– 4.70	1.49	– 6.51	6.11	1.81	2.71
5.95	9.52	– 4.65	3.18	– 5.75	3.02	1.11	2.92

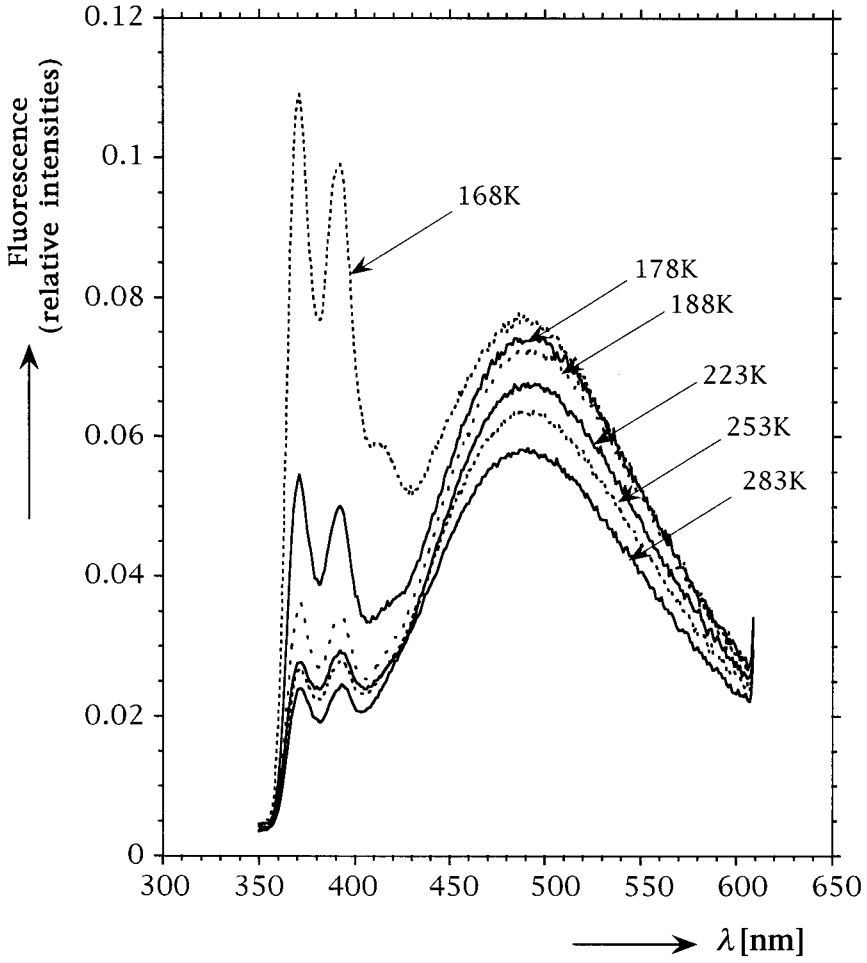

Fig. 2. *Fluorescence emission of* **1** *in butyronitrile solution at different temperatures*

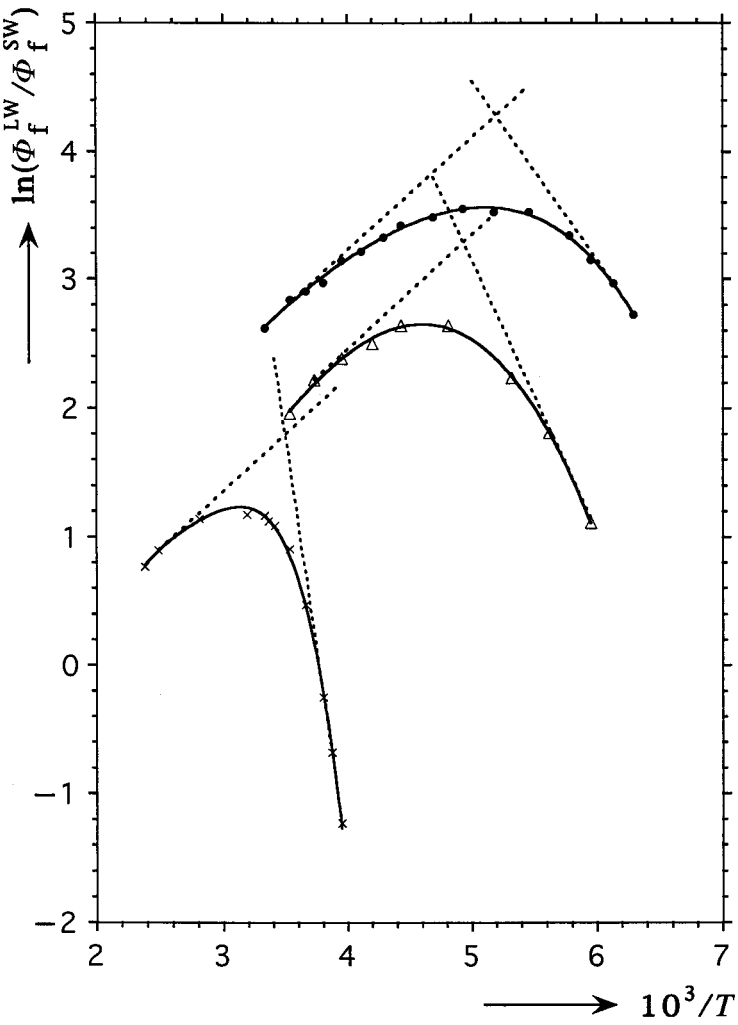

Fig. 3. *Plot of ln* (Φ_f^{LW}/Φ_f^{SW}) vs. *1/*T *in butyronitrile* (△), *Et_2O* (○), *and in GTA* (×) *solution for* **1**

3.3.2. *Et_2O Solution.* The experiments performed in this solvent were carried out in the 300 – 160 K temperature range. The value of the decay of the long-lived component of the short-wavelength emission could be obtained only at the lowest (160 K) temperature due to the weakness of the signal. When measurable, its decay parameter is the same as that of the long-wavelength emission.

As the temperature decreases, the fluorescence quantum yield of the LW* state increases, reaches a maximum around 190 K, and decreases below this temperature (*Table 3*) while its decay slows continuously from 300 K to 163 K. On the other hand, the fluorescence quantum yield of the SW* state first decreases, reaches a minimum, and begins to increase below 220 K. The position of the SW* fluorescence band is shifted by $\Delta\bar{\nu} \sim 260\ cm^{-1}$ (from 363.5 to 367 nm) when the temperature is decreased

Table 3. *Fluorescence Data of* **1** *in Et_2O Solution at Various Temperatures*

$10^3/T$	Φ_f^{LW} ($\times 10^3$)	$\ln \Phi_f^{LW}$	Φ_f^{SW} ($\times 10^3$)	$\ln \Phi_f^{SW}$	$\frac{\Phi_f^{LW}}{\Phi_f^{SW}}$	$\left(\ln \frac{\Phi_f^{LW}}{\Phi_f^{SW}}\right)$	τ_{LW} [ns]
3.33	8.46	– 4.77	0.76	– 7.18	13.8	2.63	1.59
3.53	11.9	– 4.43	0.73	– 7.22	16.3	2.79	–
3.66	12.6	– 4.37	0.68	– 7.28	18.5	2.92	2.42
3.80	13.6	– 4.29	0.65	– 7.33	20.9	3.03	–
3.95	13.7	– 4.29	0.59	– 7.43	23.2	3.145	2.69
4.11	14.0	– 4.27	0.56	– 7.49	25.0	3.219	–
4.29	14.5	– 4.23	0.52	– 7.56	27.9	3.328	2.89
4.43	14.7	– 4.22	0.48	– 7.64	30.6	3.422	–
4.69	14.7	– 4.22	0.45	– 7.71	32.7	3.486	2.93
4.93	15.0	– 4.20	0.43	– 7.75	34.9	3.552	–
5.18	15.0	– 4.20	0.44	– 7.73	34.1	3.529	3.18
5.46	15.0	– 4.20	0.44	– 7.73	34.1	3.529	–
5.78	15.0	– 4.20	0.53	– 7.54	28.3	3.343	3.27
5.95	14.5	– 4.23	0.62	– 7.39	23.5	3.152	–
6.13	14.2	– 4.25	0.73	– 7.22	19.5	2.968	3.45
6.29	13.9	– 4.28	0.91	– 7.00	15.3	2.726	3.44

from 283 to 220 K. For the LW* state, the emission band is red-shifted continuously from 467 to 482 nm ($\Delta\tilde{\nu} \approx 670\ cm^{-1}$) between 300 and 160 K. According to the data reported by *Liu* and *Bolton* [30], the dielectric constant of Et_2O increases from 4.6 to 6.1 as a function of this temperature decrease. The small red shift observed for the two emissions (*Fig. 4*) originates from the change in solvent polarity as deduced from the position of the emission (*Table 1*) taken at room temperature in various solvents (*Fig. 1*). On the other hand, the position of the SW band does not change below 220 K (inset in *Fig. 4*).

The fluorescence quantum yield of the two emissions, their ratio and the decay time (τ_{LW}) of the LW emission at the different temperatures are given in *Table 3*. Both the LW* fluorescence quantum yield Φ_f^{LW} and its decay T_{LW} are found to vary similarly between room temperature and 200 K. *Fig. 3* shows the plot of the logarithm of the fluorescence quantum yield ratio $\ln(\Phi_f^{LW}/\Phi_f^{SW})$ *vs.* the reciprocal of the absolute temperature.

3.3.3. *GTA Solution.* As in the other two solvents, the LW* fluorescence quantum yield of compound **1** in the viscous GTA solution varies only little with the temperature below 313 K (it fluctuates between 8×10^{-3} and 10^{-2}) and decreases above this temperature. For the SW* emission, the fluorescence quantum yield increases by a factor of 35 when the temperature decreases from 420 to 253 K (*Table 4*).

The difference between the results found for GTA and those obtained for the other two solvents has been attributed to the significant temperature dependence of GTA viscosity. Thus, for Et_2O, the viscosity is 0.24 cP at 295 K and 2.5 cP at 183 K, while, for GTA, it is already 25 cP at 295 K and higher than 500 cP at 260 K. *Fig. 5* shows the fluorescence spectra obtained for **1** in GTA at different temperatures, and *Table 4* gives the corresponding values of the LW* and SW* fluorescence quantum yields.

3.3.4. *Ratio of the LW* to SW* Fluorescence Quantum Yields.* Plotting the logarithm of the ratio of the LW* and SW* fluorescence quantum yields as a function of the reciprocal of the absolute temperature leads to bell-shaped curves in all three solvents

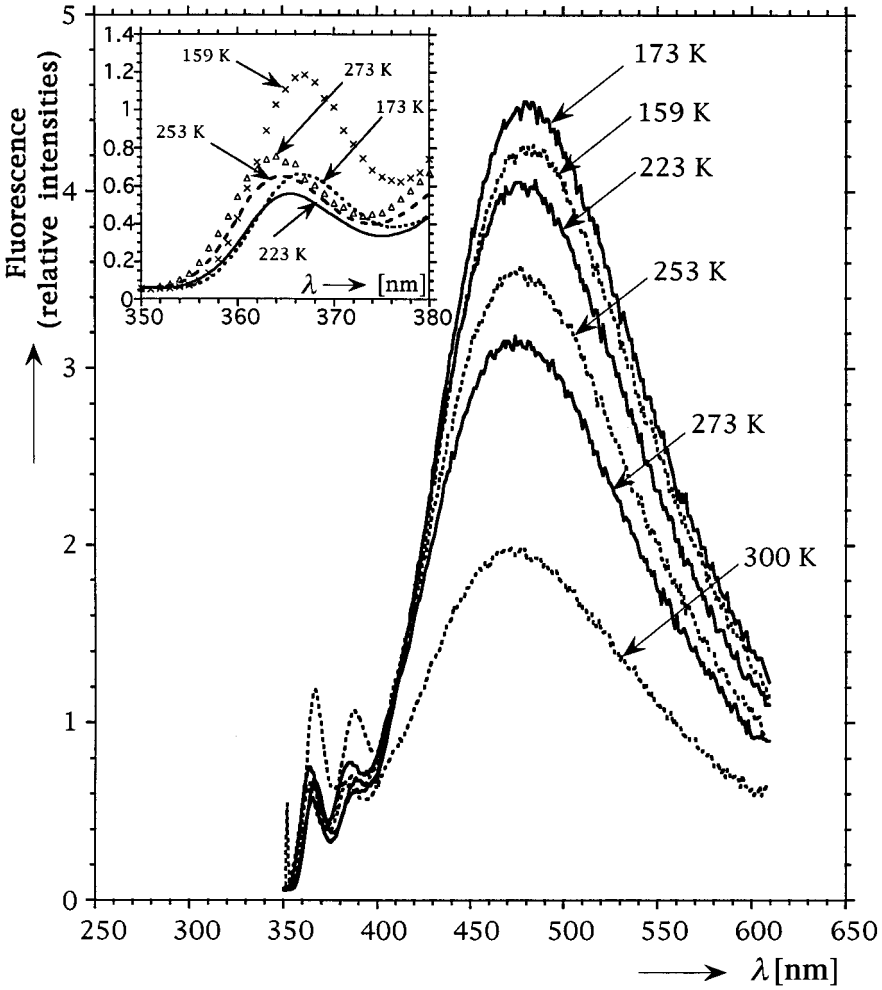

Fig. 4. *Fluorescence emission of* **1** *in* Et_2O *solution at different temperatures*

(*Fig. 3*). The value of this ratio is included in *Tables 2* to *4*. The positive slope, found at the high temperature limit of the ln (Φ_f^{LW}/Φ_f^{SW}) *vs.* 1/T curves, is *ca.* 0.88×10^3 K in the three solvents. The negative slope measured in the low-temperature range ($T < 200$ K) is -2.1×10^3 K for butyronitrile and -1.4×10^3 K for Et_2O. It is more than three times more negative (-6.6×10^3 K) in GTA in the 313 to 253 K temperature range.

The maxima of these curves, as well as the crossing point of the tangents drawn on the low and high temperature sides of the curves, show interesting features: in Et_2O and butyronitrile, the crossing point is found in the low temperature range (202 K and 192 K, respectively) while, in GTA, it appears at much higher temperature (287 K). At the same time, the (Φ_f^{LW}/Φ_f^{SW}) ratio is lower in GTA than in the other two solvents across the whole temperature range.

Table 4. *Fluorescence Data of* **1** *in GFA Solution at Various Temperatures*

T ($\times 10^3$)	$10^3/T$	Φ_f^{LW} ($\times 10^3$)	Φ_f^{SW} ($\times 10^3$)	$\frac{\Phi_f^{LW}}{\Phi_f^{SW}}$	$\left(\ln\frac{\Phi_f^{LW}}{\Phi_f^{SW}}\right)$
420	2.38	1.9	0.9	2.11	0.747
402	2.49	2.5	1.0	2.50	0.916
365	2.74	5.9	1.9	3.11	1.135
313	3.19	9.4	2.9	3.24	1.176
303	3.30	8.2	2.55	3.21	1.166
297	3.36	8.3	2.7	3.07	1.122
293	3.41	8.6	2.9	2.97	1.089
283	3.53	8.9	3.8	2.34	0.850
273	3.66	9.6	6.0	1.60	0.470
263	3.80	10.0	12.8	0.781	– 0.247
258	3.87	9.9	19.5	0.508	– 0.677
253	3.95	9.1	31.2	0.292	– 1.231

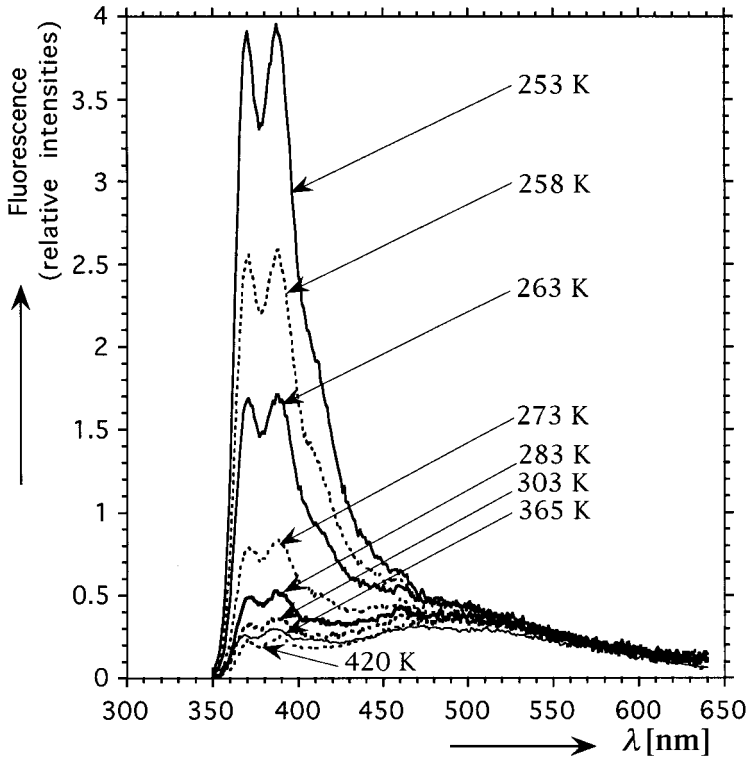

Fig. 5. *Fluorescence emission of* **1** *in GTA solution at different temperatures*

4. Discussion. – The biexponential decay curve of the SW* fluorescence has a short component, determined by the time resolution of the instrumentation, and a long component, which has the same decay parameter as that of the LW* excited-state emission. This has been taken as an argument to postulate that a reversible process is developed between the SW* and LW* excited states, although the development of the

short component of the LW* emission cannot be seen clearly because of the limited time resolution of our instrumentation.

The fluorescence emission of the SW* and LW* states evolves quite differently in butyronitrile and Et_2O solutions. Thus, when the temperature is decreased, the SW* emission first decreases until a certain temperature (different for the two solvents) is reached, and below which the emission intensity starts to increase. For the LW* excited state, both the fluorescence quantum yield and the decay time increase continuously in butyronitrile solution (see *Table 2*) while, in Et_2O, the fluorescence quantum yield first increases, reaches a maximum, and then decreases when the temperature is decreased from room temperature to 159 K.

Such behavior is typical for molecules that show dual luminescence as a result of geometric relaxation with reversible intramolecular charge transfer [16][32–36]. It also can be related to the reversible exciplex or excimer formation between two molecules, one in its excited state and the other in its ground-state [18–21][37–40]. However, the fluorescence spectrum of compound **1** shows no modification when the concentration of **1** is increased from 10^{-4} to 10^{-3} M. Furthermore, while the excimer emission originating from a triplet-triplet annihilation process has been observed already for 1,8-naphthalimides [22][42], no such emission could be detected in the 2,3-naphthalimide series.

Time-resolved fluorescence measurements with **1** at $-44°$ in MeCN solution show that the fit of the decay of the SW and LW bands with two exponential functions results in a value of -1 for the ratio of the two pre-exponential factors in the LW emission decay[2]). This demonstrates that, in a nonviscous solvent, excitation of compound **1** leads exclusively to the SW* state, which forms the LW* state according to a reversible two-state kinetics.

4.1. *Kinetics Treatment.* 4.1.1. *In Nonviscous Media.* In the case of a dual emission originating from a single molecule, as observed for compound **1**, the kinetics treatment involves the excitation of the molecule to the SW* excited state, followed by a conformational change occurring on the excited state potential-energy surface and leading to the other emitting species LW* (*Scheme 1*). When biexponential functions with identical decay parameters describe both the SW* and LW* emissions, a reversible transition between SW* and LW* can be assumed. If the ratio of the pre-exponential factors of the LW band is -1, then the kinetics can be represented by *Scheme 1*. The

Scheme 1

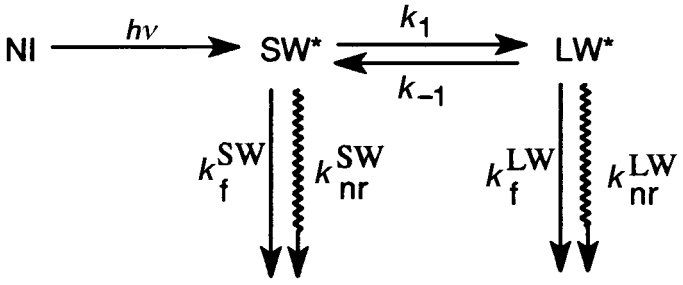

[2]) Unpublished results from the laboratory of Dr. *K. Zachariasse*, Max Planck Institut für Biophysikalische Chemie, Goettingen, Germany.

subscripts f and nr of the rate constants given in this scheme correspond to the fluorescence and the nonradiative processes, respectively. The rate constants k_1 and k_{-1} correspond to the forward and backward reactions between SW* and LW*.

The kinetic treatment of such systems has been studied in detail by various authors [12–17].

From *Scheme 1*, with the rate constants indicated above for the different pathways, the fluorescence quantum yields (Φ_f^{SW}) and (Φ_f^{LW}) of the SW* and LW* excited states, respectively, can be expressed as:

$$\Phi_f^{SW} = \frac{k_f^{SW}(k_f^{LW} + k_{nr}^{LW} + k_{-1})}{(k_f^{SW} + k_{nr}^{SW})(k_f^{LW} + k_{nr}^{LW} + k_{-1}) + k_1(k_f^{LW} + k_{nr}^{LW})} \quad (1)$$

and

$$\Phi_f^{LW} = \frac{k_f^{LW} k_1}{(k_f^{SW} + k_{nr}^{SW})(k_f^{LW} + k_{nr}^{LW} + k_{-1}) + k_1(k_f^{LW} + k_{nr}^{LW})} \quad (2)$$

The two fluorescence quantum yields have the same denominator, and their ratio leads to the simplified expression in *Eqn. 3:*

$$\frac{\Phi_f^{LW}}{\Phi_f^{SW}} = \frac{k_f^{LW}}{k_f^{SW}} \cdot \frac{k_1}{k_f^{LW} + k_{nr}^{LW} + k_{-1}} \quad (3)$$

In a nonviscous solvent like AcOEt, the viscosity varies only little over a small (*ca.* 20 K) temperature change around room temperature. As indicated ealier for **1** in this solvent, Φ_f^{SW} increases slightly (by less than 10%), while Φ_f^{LW} increases by almost 25% when the temperature is decreased from 293 K to 273 K, indicating that an *Arrhenius* energy barrier exists for at least one of the deactivation processes of the LW* state.

High-Temperature Range. In the high-temperature range, the processes originating from the SW* state are fast, as indicated by the short-lived component of its fluorescence decay in the picosecond range. Decreasing the temperature induces first a decrease of the SW* fluorescence quantum yield (*Fig. 6*), a result that we have taken as an indication that the energy barrier of the LW* → SW* reaction is higher than that of the reverse reaction. Consequently, the LW* state lies at lower energy than the SW* state.

At high temperatures, the sum of the rate constants ($k_f^{LW} + k_{nr}^{LW}$) is expected to be small compared to k_{-1}. Therefore, *Eqn. 3* can be reduced to:

$$\frac{\Phi_f^{LW}}{\Phi_f^{SW}} = \frac{k_f^{LW}}{k_f^{SW}} \cdot \frac{k_1}{k_{-1}} \quad (4)$$

Changing this expression into its logarithmic form, and taking into account that the two rate constants k_1 and k_{-1} of *Eqn. 4* are temperature sensitive and have pre-exponential factors represented by A_1 and A_{-1}, respectively, one can write:

$$\ln\left(\frac{\Phi_f^{LW}}{\Phi_f^{SW}}\right) = \ln\left(\frac{k_f^{LW}}{k_f^{SW}}\right) + \ln\left(\frac{A_1}{A_{-1}}\right) - \frac{(E_1 - E_{-1})}{RT} \quad (5)$$

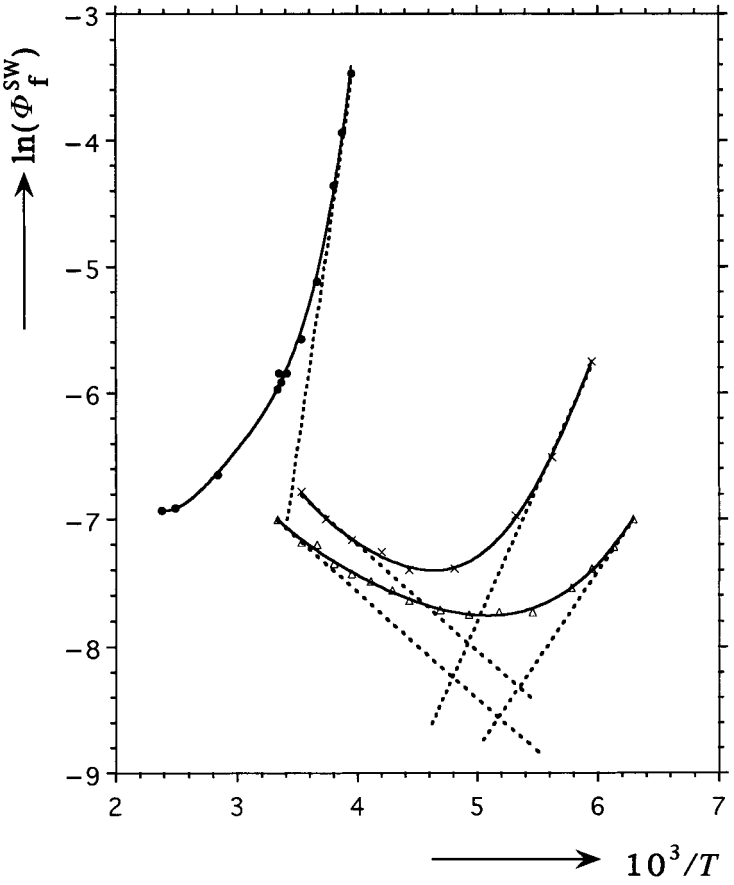

Fig. 6. *Plot of ln* (Φ_f^{SW}) vs. *1/T in butyronitrile* (×), *Et_2O* (△), *and GTA* (○) *solution for* **1**

Based on the assumption that the fluorescence rate constants k_f^{SW} and k_f^{LW} are temperature independent, and with the difference in energies defined as $E_1 - E_{-1} = \Delta H$, *Eqn. 5* becomes:

$$\ln\left(\frac{\Phi_f^{LW}}{\Phi_f^{SW}}\right) = -\frac{\Delta H}{RT} + C \tag{6}$$

The form of this equation corresponds to the linear part obtained (*Fig. 3*) in the high temperature range of the bell-shaped plots of the logarithm of the fluorescence quantum yield ratio *vs.* the reciprocal of the absolute temperature. The slope of these linear parts obtained for **1** is 0.88×10^3 K in all three solvents. It corresponds to the difference between the activation energies of the forward and backward reactions, that is to say, to the enthalpy change between the two excited states. The same ΔH value, -7.3 kJ/mol, obtained in solvents of such different polarity ($\varepsilon = 4.3$ and 19.0 for Et_2O and butyronitrile, respectively) is a consequence of the similar solvent influence on the energies of the SW* and LW* states. Since the change in dipole moment is small and

identical for the two transitions when going from the ground-state to the SW* and LW* excited states (4.5 and 4.9 D, respectively), the variation of the solvent polarity modifies the energy of the two states to a similar extent.

The energy difference $\Delta E'$ between the minimum of the ground-state potential-energy surface and the energy of the molecule on the same surface but with the geometry of the LW* excited state can be obtained easily, as it corresponds to $\Delta E' = E_1^{SW} - E_1^{LW} - \Delta H$, where E_1^{SW} is the energy of the lowest SW* singlet excited state and E_1^{LW} that of the lowest LW* excited state. The value $E_1^{SW} = 329$ kJ/mol is deduced from the intercept of the absorption and of the SW-state fluorescence bands, while the value $E_1^{LW} = 261$ kJ/mol is derived from the maximum of the LW* emission in hexane solution. Thus, the 62 kJ/mol value obtained for $\Delta E'$ clearly shows that it is the increase in the ground-state energy at the LW*-state geometry that is responsible for the strong *Stoke*'s shift observed for the LW* emission. This value is comparable to the $\Delta E' =$ 65 kJ/mol obtained for 4-(dimethylamino)benzonitrile in toluene [32], a solvent of polarity (2.38) similar to that of hexane.

Low-Temperature Range. At low temperature, the rate constant for the activated LW* → SW* reaction, k_{-1}, becomes negligible compared to $(k_f^{LW} + k_{nr}^{LW})$ and *Eqn. 3* becomes:

$$\frac{\Phi_f^{LW}}{\Phi_f^{SW}} = \frac{k_f^{LW}}{k_f^{SW}} \cdot \frac{k_1}{k_f^{LW} + k_{nr}^{LW}} \tag{7}$$

When the decay parameters obtained for the biexponential fit of the time-resolved fluorescence are very different from each other, as it is the case here (*vide supra*), then the longest of the two decay parameters can be taken as a good estimate of the $(k_f^{LW} + k_{nr}^{LW})$ sum, and, consequently, the denominator of the last part of *Eqn. 7* can be assumed to be practically constant in the temperature range of the measurements according to the values shown in *Tables 2* and *3*. Introduction of the activation parameters for k_1, and changing the relation to the logarithmic form leads to:

$$\ln\left(\frac{\Phi_f^{LW}}{\Phi_f^{SW}}\right) = \ln\left(\frac{k_f^{LW}}{k_f^{SW}}\right) + \ln\left(\frac{A_1}{k_f^{LW} + k_{nr}^{LW}}\right) - \frac{E_1}{RT} = -\frac{E_1}{RT} + C' \tag{8}$$

We assumed, as before, that the fluorescence rate constants are temperature-independent, and, based on the very small change of the longest decay parameter, we presume that the nonradiative deactivation rate constant of the LW* excited state also is independent of the temperature. Plotting the logarithm of the ratio of the fluorescence quantum yields *vs.* $1/T$ gives the curves shown in *Fig. 3*. The slope of the linear part of the curves as deduced from *Eqn. 7* in the low-temperature region is equal to -1.5×10^3 K in Et_2O and to -2.1×10^3 K in butyronitrile. These values correspond to activation energies of 12.5 kJ/mol and 17.5 kJ/mol, respectively. The activation of the viscous flow given in the literature for the two solvents in 8.6 kJ/mol [31] and 9.3 kJ/mol [42], respectively. These values obtained for E_1 in the two solvents indicate *i*) that the reaction is not controlled directly by the viscosity of the solvent, and *ii*) that the influence of the solvent polarity on the k_1 and k_{-1} reaction rates is not a consequence of a thermodynamic control since the ΔH value does not change from one solvent to the

other. The phenomenon can be understood on the basis of our model presented in previous publications [43][44] and based on *Hückel* calculations. The formation of the SW* excited state involves the transfer of electrons from the naphthalene moiety to the π^* orbital of the carbonyl groups, while the transition to the LW* state involves the shift of electrons from the *N*-phenyl moiety to the π^* orbital of the carbonyl groups. Although the scalar value of $\Delta\mu$ for the $S_o \rightarrow$ SW* and the $S_o \rightarrow$ LW* transitions are more or less the same, the angle of the dipole moment of the excited states have to be different and a polar solvent will stabilize both the SW* and the LW* excited states. Therefore, the reversible SW* $\leftrightarrow$ LW* process will involve structural changes and solvent reorganization. In a more polar solvent, the activation energies of the two reactions increase and, consequently, their rate constants are smaller. This phenomenon is observed effectively for compound **1** at room temperature in five different solvents (see *Fig. 1* and *Table 1*): the Φ_f^{LW}/Φ_f^{SW} decreases when the polarity of the solvent increases, as a result of the change in Φ_f^{SW}. Although the derivation of this quantum yield is complex, the decrease of the rate of the SW* $\rightarrow$ LW* process is expected to increase Φ_f^{SW} if one assumes that the rate constant of the competing deactivation processes of SW*, k_f^{SW} and k_{nr}^{SW}, do not change or change only little.

Table 5. *Thermodynamic Data*[a]) *of* **1** *in Butyronitrile, Et_2O and GTA solutions*

Solvent	ΔH[b]) [kJ/mol]	E_1[c]) [kJ/mol]	E[d]) [kJ/mol]
Butyronitrile	−7.3	17.5	1.1
Et_2O	−7.3	11.6	0.7
GTA	−7.3	55.0	

[a]) Taken from *Fig. 3*. [b]) Difference in enthalpy between SW* and LW*. [c]) Activation energy for the SW* to LW* transformation. [d]) Activation energy for the nonradiative deactivation of LW*.

As shown by *Stevens* and *Ban* [45], the temperature at which the ratio of the fluorescence quantum yields given in *Eqn. 3* reaches its maximum value corresponds to the temperature at which the tangents drawn at the low and high temperature sides of the curve cross each other. This occurs when

$$k_{-1} = k_f^{LW} + k_{nr}^{LW} \tag{9}$$

As the decay of the LW* state varies only little with the polarity of the solvent (*Table 1*) or with the temperature (see *Tables 2* and *3*) the rate constants k_f^{LW} and k_{nr}^{LW} are practically invariable. Therefore, the right side of *Eqn. 9* does not depend on solvent polarity and, consequently, neither does k_{-1}.

The distance Δy, between the crossing point and the point on the curve that has the same abscissa, is obtained easily by substracting the logarithm of the ratio of the fluorescence quantum yields given by *Eqn. 3* from the logarithm of the same ratio but deduced from *Eqn. 4* and taking into account *Eqn. 9* at the crossing point. This leads to the value $\Delta y = \ln 2$, identical to that expected [18][45] for a simple reversible process such as the one depicted in *Scheme 1*.

The crossing of the two tangents at the extremities of the (Φ_f^{LW}/Φ_f^{SW}) *vs.* $1/T$ plots is found at 192 K in Et_2O, 203 K in butyronitrile, and 287 K in GTA. At these temperatures, $k_{-1} = (k_f^{LW} + k_{nr}^{LW})$ and corresponds to the reciprocal of the intrinsic lifetime of the LW* state in the absence of a reverse reaction. From the logarithmic form of the *Arrhenius* expression of k_{-1} given in *Eqn. 9*, and for which we can assume that the pre-exponential factor does not vary or varies only little from one solvent to the other, it can be deduced that the temperature at which the slopes cross each other varies in the same direction as the activation energy itself.

The evolution of the curves shown in *Fig. 1* for **1** at room temperature indicates that, in the nonviscous solvents, the (Φ_f^{LW}/Φ_f^{SW}) ratio decreases when the solvent polarity increases. This behavior is the opposite of that found for 4-(dimethyl)amino-benzonitrile (DMABN) for which this ratio increases with the polarity of the solvent as demonstrated [46] by increasing the amount of propionitrile in a hexane/propionitrile mixture, the polarity of the later being much higher, 27.2, than that of the former, 1.89. This major difference between **1** and DMABN probably originates from the large difference in dipole moment of their LW* excited states. In addition, the dipole-moment vector of the ground-state and that of the SW* and LW* states point in the same direction for DMABN while, in the case of **1**, the vectors of the SW* and LW* excited states point probably in opposite directions [43][44].

4.1.2. *High-Viscosity Medium.* In the viscous GTA medium, a slight decrease in temperature induces a large increase in viscosity of the medium. We have reported in previous publications the time-resolved fluorescence decay of **1** [10] (in GTA) and **2** [11] (in various glycerol-EtOH mixtures) at low temperature and have shown their different behaviors in comparison to that in MeCN. The decrease of the k_1 and k_{-1} with temperature results from the increased steric hindrance to the rotation of the *N*-phenyl ring in both SW* → LW* and LW* → SW* steps. Simultaneously the decay of the two excited states is expected to be slowed. Effectively, the fluorescence of both SW* and LW* states of **1** decays on a relatively long time scale at low temperature, and no reversible process has been observed between the two excited states. The same behavior was found for **2** in highly viscous media [11]. This led us to use *Scheme 2*, which was already discussed in our previous articles, to explain the behavior of **1** in GTA at low temperature.

In this scheme, F* corresponds to the *Franck-Condon* level reached by excitation of the ground-state molecule. *Eqns. 1* and *2* are no longer valid for *Scheme 2*, as one must take into account the formation of the SW* and LW* states from F*. Taking the total number of molecules that form SW* and LW* as unity, one can write:

$$\alpha = \frac{k_{SW}}{k_{SW} + k_{LW}} \quad \text{and} \quad 1 - \alpha = \frac{k_{LW}}{k_{SW} + k_{LW}}$$

Following the classical steady-state kinetic expressions for the formation and the deactivation of the various excited species, the fluorescence quantum yield of state SW*, Φ_f^{SW}, can be expressed as:

$$\Phi_f^{SW} = k_f^{SW} \frac{\alpha(k_f^{LW} + k_{nr}^{LW}) + k_{-1}}{(k_f^{SW} + k_{nr}^{SW})(k_f^{LW} + k_{nr}^{LW} + k_{-1}) + k_1(k_f^{LW} + k_{nr}^{LW})} \tag{10}$$

Scheme 2

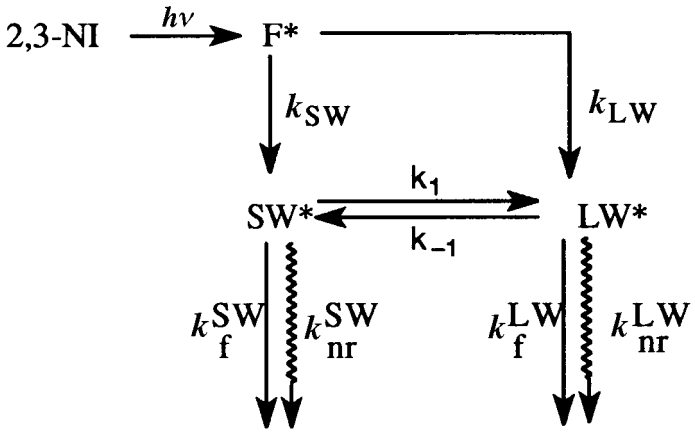

Similarly, the fluorescence quantum yield of the LW* state, Φ_f^{LW}, is expressed as:

$$\Phi_f^{LW} = \frac{k_f^{LW}(1 - \alpha)(k_f^{SW} + k_{nr}^{SW}) + k_1}{(k_f^{SW} + k_{nr}^{SW})(k_f^{LW} + k_{nr}^{LW} + k_{-1}) + k_1(k_f^{LW} + k_{nr}^{LW})} \tag{11}$$

The ratio of the two fluorescence quantum yields gives the reduced expression in *Eqn. 12:*

$$\frac{\Phi_f^{LW}}{\Phi_f^{SW}} = \frac{k_f^{LW}}{k_f^{SW}} \cdot \frac{(1 - \alpha)(k_f^{SW} + k_{nr}^{SW}) + k_1}{\alpha(k_f^{LW} + k_{nr}^{LW}) + k_{-1}} \tag{12}$$

At low temperature, k_{-1} can be neglected compared to $\alpha(k_f^{LW} + k_{nr}^{LW})$ (*vide supra*). If one wants to understand the meaning of the steep linear slope of the *Steven* and *Ban* plot in the low-temperature region of the curve of **1** in GTA, further simplifications have to be made in the numerator of *Eqn. 12*. Time-resolved experiments carried out with **1** in the picosecond time scale at low temperature in GTA solution shows no development on the LW* emission that appears simultaneous to the laser pulse, as does the SW* emission. As a consequence, one can assume that the k_1 of the SW* → LW* process is negligible compared to the rate constants of the other processes that deactivate SW*, *i.e.*, internal conversion ($k_{ic}^{SW} = k_f^{SW} + k_{nr}^{SW}$), the main deactivation channel [43]. If one admits that α does not change much in the temperature range of the investigations, then *Eqn. 12* simplifies to:

$$\frac{\Phi_f^{LW}}{\Phi_f^{SW}} = \frac{k_f^{LW}}{k_f^{SW}} \cdot \frac{(1 - \alpha)k_{ic}^{SW}}{\alpha(k_f^{LW} + k_{nr}^{LW})} \tag{13}$$

and by changing k_{ic}^{SW} to $A_{ic}^{SW} e^{-\frac{\Delta E_{ic}^{SW}}{RT}}$ and taking the logarithmic form, one obtains *Eqn. 14:*

$$\ln \frac{\Phi_f^{LW}}{\Phi_f^{SW}} = \ln \left(\frac{k_f^{LW}(1 - \alpha)A_{ic}^{SW}}{k_f^{SW}\alpha(k_f^{LW} + k_{nr}^{LW})} \right) - \frac{\Delta E_{ic}^{SW}}{RT} = -\frac{\Delta E_{ic}^{SW}}{RT} + C \tag{14}$$

For the fluorescence quantum yields, either both increase with the excited state lifetime, or one increases at the expense of the other. The Φ_f^{SW} value increases effectively by more than one order of magnitude (*Table 4*) when the temperature of the GTA solution is decreased from 313 to 253 K but Φ_f^{LW} is found to be practically invariant in this temperature range. A similar result was obtained when the viscosity was changed by applying a high pressure over the solution at room temperature [29]. For the SW* state, the position and the shape of its fluorescence emission varies only little with the substitution on the *N*-phenyl ring [10] and its spectra overlaps that of 2-methylbenzo[*f*]isoindole-1,3-dione, thus verifying that the transition is located in the naphthalimide moiety. Therefore, **1** must behave similarly to **2**, corroborating that its kinetics follows the three-level scheme [11] depicted in *Scheme 2*.

In the case of the GTA solution of **1**, the bell-shaped ln (Φ_f^{LW}/Φ_f^{SW}) *vs.* $1/T$ curve is shifted to higher temperatures (*Fig. 3*) and the slope of the curve in the low temperature range (between 313 and 253 K) is -6.6×10^3 K. It corresponds to a 55 kJ/mol activation energy. Previous experiments by *Von Salis* and *Labhart* [47] have shown that the logarithm of the viscosity of GTA plotted against the reciprocal of the temperature deviates from linearity. On the other hand, *Braun* and *Rettig* [48] have pointed out that a single value cannot be given for its viscous-flow activation energy. They evaluated an average value $E_\eta > 50$ kJ/mol for GTA. This high viscosity effect may act upon two different processes: *i*) blocking of the F* → LW* and SW* → LW* paths, but one would have expected complete disappearance of the SW* state and of its fluorescence emission, and, as it has been already pointed out above, this hypothesis can be excluded since the LW* state fluorescence remains unchanged when the viscosity is increased. *ii*) The other assumption is connected with the internal conversion of the SW* state to the ground state. We know already that a *t*-Bu substituent at position 2 on the phenyl ring attached to the N-atom of **2** prevents the formation of the LW* state and that the SW* state decays monoexponentially and in the ns time scale [11]. Behavior similar to that found for **1** is observed with **2** when the temperature is decreased: in GTA the SW* fluorescence increases strongly while that of the LW* state varies only little and is still present at low temperature. The decay of the SW* excited state of **2** becomes instructive: at 283 K, it is shorter than 0.2 ns and it increases up to 4.4 ns when the temperature is decreased to 233 K. The same trend is observed for compound **1**, but the analysis was perturbed by an inpurity present in GTA and absorbing at the laser excitation wavelength (296 nm), a position where **1** absorbs very weakly. We have already observed such evolution and have attributed it to a conformational change occurring in the excited state and, more precisely, to the inversion of the N-atom [22]. This can be correlated also to the pyramidalization of the N-atom described by *Lopez-Arbelao et al.* as an umbrella-like motion (ULM) in the case of xanthenes [49] and rhodamines [50]. The same influence of the pyramidalization of the N-atom on the formation of the charge-transfer excited state from the local excited state has been emphasized by *Zachariasse* and co-workers [51] in the case of 4-(*N*,*N*-dimethylamino)benzonitrile and derivatives. A *Gibbs* energy of activation $\Delta G^{\ddagger}$ of *ca.* 36 kJ/mol^{-1} has been measured by *Lehn* and *Wagner* [52] for the inversion of the pyramidal shape of ground-state amines (flip-flop motion). They also reported that a decrease of the temperature to 164 K blocks this inversion. Consequently, one can

attribute the important increase of the SW* emission of **1** and **2** to the progressive suppression of the inversion process of their N-atoms.

LW State Internal Conversion.* In the region where the ln (Φ_f^{LW}/Φ_f^{SW}) *vs.* $1/T$ curve begins to decrease, at $10^3/T > 4.7$ K^{-1} in butyronitrile and > 5.1 K^{-1} in Et_2O, the decay of the LW state varies only little, by $< 15\%$ in butyronitrile and $< 10\%$ in Et_2O. The expression $1/(k_f^{LW} + k_{nr}^{LW} + k_{-1})$ can be approximated roughly to the lifetime of the LW* excited state. At low temperature, k_{-1} is negligible, as already indicated (*vide supra*). Therefore, the fluorescence decay time of the LW* state corresponds to $1/(k_f^{LW} + k_{nr}^{LW})$. Because of the low fluorescence quantum yield of the LW* state, k_f^{LW} can be neglected compared to k_{nr}^{LW}. Thus, the small temperature dependence of τ_{LW} can be attributed to the radiationless deactivation of the LW* state. Plotting ln ($1/\tau_{LW}$) as a function of $1/T$ in the low-temperature range gives a straight line with a slope of -0.09×10^3 K for Et_2O and of -0.14×10^3 K for butyronitrile. These values correspond to activation energies as little as 0.7 and 1.1 kJ/mol, respectively, corroborating the negligible influence of the temperature upon the nonradiative deactivation of the LW* excited state.

5. Conclusion. – We have shown that, contrary to results obtained with **2**, which is unsubstituted on its *N*-phenyl ring and shows no reversibility between its SW* and LW* excited states, the depopulation of the singlet excited state of **1** involves a reversible process in solvents of low or moderate viscosity. The polarity dependence of the ratio of the SW* and LW* fluorescence at room temperature, as well as the change with solvent polarity of the activation energy for the SW* $\rightarrow$ LW* reaction, shows that the resolvation of the excited molecules constitutes an important factor in the photophysics of **1** in nonviscous media. However, in the viscous GTA solvent, the reversibility between the two excited states of molecule **1** has been observed only at high temperature when the viscosity of the solvent has been reduced. The principal changes that are observed in the fluorescence spectra upon lowering the temperature are relevant to the SW* state, the internal conversion of which is strongly influenced by the effect of the viscosity on the vibrational movement of the N-atom.

This work was supported by a scientific exchange program between the *Hungarian Committee for Technological Development* and the *French Ministry of Foreign Affairs* (*Balaton Project* 98005), and by the *Hungarian Science Foundation* (OTKA, project T 033102).

REFERENCES

[1] I. Saito, M. Takayama, *J. Am. Chem. Soc.* **1995**, *117*, 5590.
[2] I. Saito, M. Takayama, H. Sugiyama, K. Nakatani, A. Tsuchida, M. Yamamoto, *J. Am. Chem. Soc.* **1995**, *117*, 6406.
[3] I. Saito, M. Takayama, H. Sugiyama, T. Nakamura, in 'DNA and RNA Cleavers and Chemotherapy of Cancer and Viral Diseases', Ed. B. Meunier, Kluwer Academic Publishers, 1996, p. 163.
[4] P. F. Bousquet, M. F. Brana, D. Conlon, K. M. Fitzgerald, D. Perron, C. Cocchiaro, R. Miller, M. Moran, J. George, X. D. Qian, G. Keilhauser, C. A. Romerdahl, *Cancer Res.* **1995**, *55*, 1176.
[5] M. F. Brana, J. M. Castellano, M. Moran, M. J. Perez de Vega, X. D. Qian, C. A. Romerdahl, G. Keilhauser, *Eur. J. Med. Chem.* **1995**, *30*, 235.
[6] R. J. Hodgkiss, G. W. Jones, A. Long, R. W. Middletown, J. Parrick, M. R. L. Sreatford, P. Wardman, G. D. Wilson, *J. Med. Chem.* **1991**, *34*, 2268.
[7] B. A. Hayes, S. Gupta, S.-C. Chang, R. E. Utecht, D. E. Lewis, *J. Labelled Compd. Radiopharm.* **1996**, *38*, 607.
[8] S.-C. Chang, B. J. Archer, R. E. Utecht, D. E. Lewis, M. M. Judy, J. L. Matthews, *Biomed. Chem. Lett.* **1993**, *3*, 555.

[9] T. C. Chang, D. E. Lewis, J. S. Allan, F. Sogarandes-Bernal, R. E. Utech, M. M. Judy, J. L. Matthews, *AIDS Res. Hum. Retroviruses* **1993**, *9*, 891.
[10] V. Wintgens, P. Valat, J. Kossanyi, A. Demeter, L. Biczòk, T. Bérces, *J. Photochem. Photobiol. A.* **1996**, *93*, 109.
[11] P. Valat, V. Wintgens, J. Kossanyi, L. Biczòk, A. Demeter, T. Bérces, *J. Am. Chem. Soc.* **1992**, *114*, 947.
[12] M. C. C. de Lange, D. Thorn Leeson, K. A. B. van Kuijk, A. H. Huizer, C. A. G. O. Varma, *Chem. Phys.* **1993**, *174*, 425; M. C. C. de Lange, D. Thorn Leeson, K. A. B. van Kuijk, A. H. Huizer, C. A. G. O. Varma, *Chem. Phys.* **1993**, *177*, 243.
[13] T. Asahi, M. Ohkohchi, R. Matsusaka, N. Mataga, R. P. Zhang, A. Osuka, K. Maruyama, *J. Am. Chem. Soc.* **1993**, *115*, 425.
[14] M. van der Auweraer, Z. R. Grabowski, W. Rettig, *J. Phys. Chem.* **1991**, *95*, 2083.
[15] M. van der Auweraer, A. Gilbert, F. C. de Schryver, *J. Phys. Chem.* **1981**, *85*, 3198.
[16] Z. R. Grabowski, K. Rotkiewicz, A. Siemiarczuk, D. Cowley, W. Baumann, *Nouv. J. Chim.* **1979**, *3*, 443.
[17] J. B. Birks, in 'Photophysics of Aromatic Molecules', Ed. J. B. Birks, Wiley, London, 1970, Vol. 2, p. 453.
[18] K. A. Zachariasse, *Trends Photochem. Photobiol.* **1994**, *3*, 211.
[19] F. Meeus, M. van der Auweraer, F. C. de Schryver, *J. Am. Chem. Soc.* **1980**, *102*, 4071.
[20] F. Meeus, M. van der Auweraer, J. C. Dederen, F. C. de Schryver, *Rec. Trav. Chim. Pays-Bas* **1979**, *98*, 220.
[21] H. Knibbe, D. Rehm, A. Weller, *Ber. Bunsen-Ges. Phys. Chem.* **1969**, *73*, 839.
[22] V. Wintgens, P. Valat, J. Kossanyi, L. Biczòk, A. Demeter, T. Bérces, *J. Chem. Soc. Faraday Trans.* **1994**, *90*, 411.
[23] P. Valat, S. Tripathi, V. Wintgens, J. Kossanyi, *New J. Chem.* **1990**, *14*, 825.
[24] G. Hui Bon Hoa, C. Di Primo, I. Dondaine, S. G. Sligar, I. C. Gunsalus, P. Douzou, *Biochemistry* **1989**, *28*, 651.
[25] G. Hui Bon Hoa, P. Douzou, N. Dahan, C. Balny, *Anal. Biochem.* **1982**, *120*, 125.
[26] E. Lippert, *Z. Naturforsch.* **1955**, *10A*, 541.
[27] N. Mataga, Y. Kaifu, M. Koizumi, *Bull. Chem. Soc. Jpn.* **1955**, *28*, 690.
[28] J. T. Edwards, *J. Chem. Educ.* **1970**, *47*, 261.
[29] G. Hui Bon Hoa, J. Kossanyi, V. Wintgens, A. Demeter, L. Biczòk, T. Berces, in preparation.
[30] J. Y. Liu, J. R. Bolton, *J. Phys. Chem.* **1992**, *96*, 1718.
[31] 'Landolt-Bornstein', Springer Verlag Berlin, 1959, Bd. 2, Vols. 6 and 8.
[32] Y. Il'ichev, W. Kühnle, K. Zachariasse, *J. Phys. Chem.* **1998**, *102*, 5670.
[33] U. Leinhos, W. Kühnle, K. Zachariasse, *J. Phys. Chem.* **1991**, *95*, 2013.
[34] G. Pontérini, J.-C. Mialocq, *New J. Chem.* **1989**, *13*, 157.
[35] M. Van der Auweraer, A. Vannereau, F. de Schryver, *J. Mol. Struct.* **1982**, *84*, 343.
[36] W. Rettig, *J. Lumin.* **1980**, *26*, 21.
[37] D. O'Connor, W. R. Ware, *J. Am. Chem. Soc.* **1976**, *98*, 4722.
[38] M. H. Hui, W. R. Ware, *J. Am. Chem. Soc.* **1976**, *98*, 4706.
[39] A. E. W. Knight, B. K. Selinger, *Austr. J. Chem.* **1971**, *10*, 43.
[40] J. D. Birks, D. J. Dyson, I. H. Munro, *Proc. R. Soc., London* **1963**, *Ser. 275*, 575.
[41] T. C. Barros, P. Berci Filho, V. G. Toscano, M. J. Politi, *J. Photochem. Photobiol., A.* **1995**, *89*, 141.
[42] J. A. Riddick, A. Weissberger, W. B. Bunger, 'Techniques of Chemistry, Organic Solvents: Physical Properties and Methods of Purification', Vol. 2, 3rd edn., John Wiley and Sons, Inc., New York, 1970.
[43] A. Demeter, T. Bérces, L. Biczòk, V. Wintgens, P. Valat, J. Kossanyi, *J. Phys. Chem.* **1996**, *100*, 2001.
[44] V. Wintgens, P. Valat, J. Kossanyi, A. Demeter, L. Biczòk, T. Bérces, *New J. Chem.* **1996**, *20*, 1149.
[45] B. Stevens, M. I. Ban, *Trans. Faraday Soc.* **1964**, *60*, 1515.
[46] A. Nag, T. Kundu, K. Bhattacharyya, *Chem. Phys. Lett.* **1989**, *160*, 257.
[47] G. A. Von Salis, H. Labhart, *J. Phys. Chem.* **1969**, *73*, 752.
[48] D. Braun, W. Rettig, *Chem. Phys.* **1994**, *180*, 231.
[49] F. Lòpez-Arbeloa, I. Urrecha-Aguirresacona, I. Lòpez-Arbeloa, *Chem. Phys.* **1989**, *130*, 371.
[50] F. Lòpez-Arbeloa, T. Lòpez-Arbeloa, P. Hernandez-Bartolomé, M. J. Tapia-Estévez, I. Lòpez-Arbeloa, *Proc. Indian Acad. Sci.* **1992**, *104*, 165.
[51] a) T. von der Haar, A. Hebecker, Y. Il'ichev, Y.-B. Jiang, W. Kühnle, K. A. Zachariasse, *Recl. Trav. Chim. Pays-Bas* **1995**, *114*, 430; b) K. A. Zachariasse, T. von der Haar, U. Leinhos, W. Kühnle, *J. Inf. Rec. Mats.* **1994**, *21*, 501; c) K. A. Zachariasse, T. von der Haar, A. Hebecker, U. Leinhos, W. Kühnle, *Pure Appl. Chem.* **1993**, *65*, 1745.
[52] J. M. Lehn, J. Wagner, *Tetrahedron* **1970**, *26*, 4227.

Received May 9, 2001